Neurobiology of Aging 34 (2013) 2023–2036

Contents lists available at SciVerse ScienceDirect

Neurobiology of Aging

journal homepage: www.elsevier.com/locate/neuaging

Review

Alzheimer's disease: connecting findings from graph theoretical studies of brain networks

Betty M. Tijms [a,*], Alle Meije Wink [b], Willem de Haan [a], Wiesje M. van der Flier [a,c], Cornelis J. Stam [d], Philip Scheltens [a], Frederik Barkhof [b]

[a] Alzheimer Center and Department of Neurology, VU University Medical Center, Amsterdam, the Netherlands
[b] Department of Radiology, VU University Medical Center, Amsterdam, the Netherlands
[c] Department of Epidemiology and Biostatistics, VU University Medical Center, Amsterdam, the Netherlands
[d] Department of Clinical Neurophysiology and MEG, VU University Medical Center, Amsterdam, the Netherlands

ARTICLE INFO

Article history:
Received 10 October 2012
Received in revised form 19 February 2013
Accepted 25 February 2013
Available online 28 March 2013

Keywords:
Dementia
Graph theory
Connectivity
Brain networks
MRI
DTI
EEG
MEG

ABSTRACT

The interrelationships between pathological processes and emerging clinical phenotypes in Alzheimer's disease (AD) are important yet complicated to study, because the brain is a complex network where local disruptions can have widespread effects. Recently, properties in brain networks obtained with neuroimaging techniques have been studied in AD with tools from graph theory. However, the interpretation of graph alterations remains unclear, because the definition of connectivity depends on the imaging modality used. Here we examined which graph properties have been consistently reported to be disturbed in AD studies, using a heuristically defined "graph space" to investigate which theoretical models can best explain graph alterations in AD. Findings from structural and functional graphs point to a loss of highly connected areas in AD. However, studies showed considerable variability in reported group differences of most graph properties. This suggests that brain graphs might not be isometric, which complicates the interpretation of graph measurements. We highlight confounding factors such as differences in graph construction methods and provide recommendations for future research.

1. Introduction

Alzheimer's disease (AD) is a progressive, disabling neurodegenerative disorder that accounts for approximately 50%–80% of all dementia cases. AD is histopathologically defined by the presence of amyloid-β plaques and tau-related neurofibrillary tangles. These plaques and tangles have been associated with local synaptic disruptions, suggesting that AD is a dysconnectivity disease (Arendt, 2009; Blennow et al., 1996; Delbeuck et al., 2003; Takahashi et al., 2010). At later stages of the disease, cortical atrophy progresses in an orderly fashion from subcortical structures such as the hippocampus into associative cortical areas and finally primary sensory areas (Braak and Braak, 1991; Jack et al., 2010). These observations suggest that specific cortical areas are vulnerable for AD pathology, which may determine how the disease propagates along specific paths in a network. If AD is indeed a dysconnectivity disease then this can only be captured with a network approach, because the structural elements of the brain form an intricate network at different spatial scales (ranging from neurons to anatomical regions) from which functional dynamics emerge. Local disruptions in such complex networks can have unpredictable and widespread effects (see e.g., Gratton et al., 2012).

Graph theory provides tools to concisely quantify the properties of complex networks that describe interrelationships (represented by edges) between objects (represented by nodes; see Section 2 for an explanation of graph theoretical concepts). It has been proposed that a detailed understanding of structural connectivity between cortical areas (i.e., the 'human connectome') will provide a mechanistic understanding of the dynamic function that can emerge (Sporns et al., 2005). Graph theory offers at least 2 important advantages in comparison with other network approaches. First, it provides for each node quantitative measurements that incorporate connectivity information from the complete network, reflecting the

* Corresponding author at: Alzheimer Center and Department of Neurology, VU University Medical Center, PO Box 7057, 1007 MB Amsterdam, The Netherlands. Tel.: +31 204440816; fax: +31 204440816.
E-mail address: betty.tijms@gmail.com (B.M. Tijms).

0197-4580/$ – see front matter © 2013 Elsevier Inc. All rights reserved.
http://dx.doi.org/10.1016/j.neurobiolaging.2013.02.020

integrated nature of local brain activity. For example, hubs can be defined as nodes that make information processing in a graph more efficient and increase a network's robustness to random failure (Albert et al., 2000; see section 2). However, such nodes are also bottlenecks, because the loss of a hub is likely to fragment a network into disconnected parts. Interestingly, hubs have been associated with epidemic transfer, and might therefore be important to study how a disease propagates in a network (Pastor-Satorras and Vespignani, 2001).

A second advantage of graph theory is that it provides a general language that enables direct comparison of graphs that describe different types of data (e.g., functional connectivity vs. anatomical connectivity). For these reasons, graph theory seems to be a promising framework to disentangle how various pathological processes in AD, such as spatial patterns of cortical atrophy and functional disruptions, are associated with each other and why the disease propagates along specific routes.

Up to now graph theory has been mainly used to describe brain graphs that were obtained with anatomical, morphological, and functional neuroimaging techniques, because a detailed a description of the human connectome is difficult to obtain (for reviews see Bassett and Bullmore, 2006; Bullmore and Bassett, 2011; Bullmore and Sporns, 2009, 2012, 2013; Stam and Reijneveld, 2007). It has been argued that if graphs constructed from different imaging modalities reflect true brain connectivity, they should have corresponding network topologies. Yet, it is still an open question whether connectivity as defined across neuroimaging modalities measure the same underlying construct (although associations across modalities have been reported: Gong et al., 2012; Honey et al., 2007, 2009).

Recently, brain networks in AD have been investigated by applying the theoretical framework of graph theory to neuroimaging data (Çiftçi, 2011; de Haan et al., 2009, 2012b, 2012c; He et al., 2008; Li et al., 2012; Lo et al., 2010; Sanz-Arigita et al., 2010; Stam et al., 2009; Supekar et al., 2008; Tijms et al., 2013; Yao et al., 2010; Zhao et al., 2012. For AD-specific reviews see: He et al., 2009; Xie and He, 2012; and for neurodegenerative diseases in general, see: Greicius and Kimmel, 2012). Importantly, these studies have reported altered local and global graph properties in AD, supporting the clinical relevance of brain graphs. However, the interpretation of 'disturbance' might be ambiguous, because the definition for connectivity depends on the imaging modality used.

It could be hypothesized that if brain graphs are robust across neuroimaging modalities and of an isometric nature, then group differences in graph measurements between AD and control subjects should converge across studies. Here we investigate this question by reviewing graph studies in AD and we will introduce a heuristically defined graph space to investigate which theoretical models best explain converging network alterations.

2. Studies of AD and graph theory

A literature search was carried out in the following online resources: PubMed, Web of Science, and Google Scholar. Combinations of the following key words were used: structural magnetic resonance imaging (sMRI), functional magnetic resonance imaging (fMRI), diffusion tensor imaging (DTI), diffusion spectrum imaging (DSI), EEG (electroencephalography), magnetoencephalography (MEG), gray matter, white matter, connectivity, AD, networks, small world. From this search articles were selected that used graph theory to analyze networks at the whole-brain level and that reported the network size and connectivity density (i.e., the ratio of the number of existing connections to maximum possible number of connections). Table 1 shows an overview of the studies found.

2.1. Graph theoretical concepts

The building blocks of networks are nodes (i.e., vertices) that represent the objects of interest and the edges that connect them. Presently, no general consensus exists as to how to best choose nodes and a connectivity function, mostly because the exact mapping of neuronal connectivity at the cell and/or population level to the macroscopic level of neuroimaging data is unknown (Bullmore and Sporns, 2009; Rubinov and Sporns, 2010; Sporns, 2011; Sporns et al., 2005).

Nodes in all brain graphs represent anatomical areas. Table 2 shows that network sizes varied across studies from 21 (EEG) to 8683 (sMRI). In magnetic resonance imaging (MRI) research, most studies have defined nodes using 90 regions from the Automated Anatomical Labeling atlas (AAL) (Tzourio-Mazoyer et al., 2002), apart from Lo et al. (2010), who used 78 AAL regions, He et al. (2008), who used 54 regions defined with automated nonlinear image matching and anatomical labeling software (Collins et al., 1995), and Tijms et al. (2013), who used a template-free approach resulting in an average graph size of 8683 nodes.

Edges connect nodes according to some connectivity function: the existence and/or integrity of a DTI traced white matter tract, temporal associations (measured with either linear or nonlinear techniques in fMRI, MEG, and EEG) or covariation of cortical thickness or volume between anatomical areas across subjects (sMRI) or similarity of cortical structure within an individual (sMRI). In graph theoretical context the term 'connection' indicates the existence of an edge, which in sMRI and functional networks might exist in the absence of white matter tracts. Defining the relationships between nodes is not a trivial task, because even within a modality different association metrics can lead to different connectivity patterns (see Liang et al., 2012; Smith et al., 2011). Preprocessing procedures can also influence connectivity. For example, spatial smoothing of signals to reduce the influence of normalization errors introduces (spurious) correlations between spatially nearby voxels (Li et al., 2012; Supekar et al., 2008; Yao et al., 2010).

Finally, the edges can be weighted, thresholded weighted, and unweighted (i.e., binarized). In contrast to binarized networks, weighted networks convey information about the strength of connectivity, including weak relationships that might even be spurious (introducing noise into the network). Weak relationships are given 0 weight in thresholded networks, but setting a threshold involves an arbitrary decision. Therefore, topologies of thresholded networks are usually studied for a range of different threshold values. When studying patient populations, including AD, a priori group differences in global connectivity will introduce group differences in connectivity densities of weighted and unweighted networks, complicating group comparisons of other graph properties.

2.2. A heuristic model of graph space

The studies in this review investigated 13 different graph properties in total, which are illustrated in Fig. 1 along with the theoretical models that explain them (for more details see Table 3. Readers unfamiliar with graph theoretical concepts are referred to Section 1 of the Supplementary data).

These graph properties derive their meaning from the fact that they are defined in the context of specific structural models of complex networks, from which functional dynamics can emerge. However, the precise structural description, also called the 'connectome', of the human brain is largely unknown, because at different spatial scales it is difficult to measure; at the micro level of neurons, their sheer number hinders the mapping of all synaptic

Table 1
Sample characteristics of graph theoretical studies on Alzheimer's disease

Study	Modality	Group	Subjects, *n* (F)	Age, mean y (± SD)	Age range, y	Mean MMSE score (± SD or range)	Task
1. Stam et al., 2007	EEG	AD	15 (11)	69.6 (7.9)	54–77	21.4 (4)	Resting state
		C	15 (9)	70.6 (7.9)	57–78	28.4 (1.1)	Resting state
2. de Haan et al., 2009	EEG	AD	20 (13)	65.5 (—)	51–76	21.5 (14–27)	Resting state
		FTLD	15 (3)	63 (—)	43–79	24.5 (13–30)	Resting state
		C	23 (9)	59 (—)	49–78	29 (27–30)	Resting state
3. Stam et al., 2009	MEG	AD	18 (11)	72.1 (5.6)	nr	19.2 (13–25)	Resting state
		C	18 (11)	69.1 (6.8)	nr	29 (27–30)	Resting state
4. de Haan et al., 2012c	MEG	AD	18 (6)	67 (9)	nr	23 (1)	Resting state
		C	18 (11)	66 (9)	nr	29 (1)	Resting state
5. Supekar et al., 2008	fMRI	AD	21 (11)	63.97 (—)	48–83	22.14 (12–29)	Resting state
		C	18 (8)	62.84 (—)	37–77	29 (27–30)	Resting state
6. Sanz-Arigita et al., 2010	fMRI	AD	18 (9)	70.7 (7.2)	59–79	22.6 (3.2)	Resting state
		C	21 (13)	70.7 (6)	60–81	28.7 (1.4)	Resting state
7. Çiftçi, 2011	fMRI	AD	13 (7)	77.2 (—)	66–82	nr	Finger press task
		C	14 (9)	74.9 (—)	66–89	nr	Finger press task
		Y	14 (9)	21.1 (—)	18–24	nr	Finger press task
8. Zhao et al., 2012	fMRI	AD	33 (20)	66.2 (9.4)	nr	15.3 (3.0)	Resting state
		C	20 (10)	63.0 (5.8)	nr	27.8 (1.3)	Resting state
9. Lo et al., 2010	DTI	AD	25 (10)	79.4 (5.89)	nr	20.92 (2.36)	na
		C	30 (11)	77.07 (6.37)	nr	28.83 (0.99)	na
10. He et al., 2008	sMRI	AD	92 (54)	76.65 (7.13)	62–94	24.38 (14–30)	na
		C	97 (71)	75.93 (9.03)	60–94	28.95 (25–30)	na
11. Yao et al., 2010	sMRI	AD	91 (41)	76.16 (7.81)	55–73	nr	na
		MCI	113 (34)	75.12 (7.60)	56–89	nr	na
		C	98 (49)	77.27 (4.66)	70–90	nr	na
12. Li et al., 2012	sMRI	AD	37 (14)	74.8 (8.0)	nr	23.0 (1.9)	na
		sMCI	36 (11)	75.3 (6.9)	nr	26.8 (1.6)	na
		pMCI	39 (14)	75.6 (7.4)	nr	26.5 (1.7)	na
		C	40 (17)	73.7 (6.3)	nr	29.4 (0.7)	na
13. Tijms et al., 2013	sMRI	AD	38 (19)	72.06 (4.43)	nr	19.65 (5.42)	na
		C	38 (19)	71.91 (4.43)	nr	27.67 (2.20)	na

Key: AD, Alzheimer's disease; C, control group; DTI, diffusion tensor imaging; EEG, electroencephalography; F, female; fMRI, functional magnetic resonance imaging; FTLD, frontotemporal lobar degeneration; MCI, minor cognitive impairment; MEG, magnetoencephalography; na, not applicable; nr, not reported; pMCI, progressive MCI; sMCI, stable MCI; sMRI, structural magnetic resonance imaging; Y, young control subjects.

connections, and at the macro level of neuroimaging only indirect measurements of connectivity can be obtained. It has been proposed that graph theoretical properties will help to link structure to function across different spatial and temporal scales (Deco et al., 2012; Sporns, 2013, 2011).

To date, graph theory has been mostly used to describe brain networks and a number of characteristic properties have been robustly reported: short characteristic path lengths, high local clustering, modularity, and the existence hubs. It has been suggested that the convergence of these properties across studies reflect that brain networks have evolved by optimizing multiple, possibly conflicting constraints, including: the minimization of the number of edges (which is related to minimization of building and maintenance costs) while retaining high connectivity, the energy needed for information exchange, maximization of a graph's robustness against attack (i.e., the loss of edges or nodes), and functional adaptability (e.g., Bullmore and Sporns, 2012; Chklovskii, 2004; Sporns, 2011, 2013; Stam and van Straaten, 2012; Stam et al., 2010).

The models illustrated in Fig. 1b all represent a solution to optimize one of these constraints: scale 1 is the 'information integration–segregation scale' and represents the spectrum of topologies between ordered and randomly connected graphs; scale 2 is the 'resilience against attack scale' and represents the emergence of hubs in a network; and scale 3 is the 'functional adaptability scale' that represents the existence of modules.

Scale 1 explains how a high amount of clustering can coexist with a low characteristic path length. This is explained by the 'small world' model in which random rewiring of edges in a network with a regular topology introduces shortcuts that dramatically reduces the average path length, while maintaining high clustering until the graph loses its clustering and becomes random when most connections are rewired (Watts and Strogatz, 1998). The balance of high clustering and short path lengths represents an evolutionary optimization of the balance of information segregation (nodes that form specialized clusters) and information integration (connections between clusters). An interesting property of small world networks is that the clustering coefficient is independent of network size, which has been reported for brain graphs. However, this model fails to explain the existence of hubs (i.e., degree heterogeneity).

Models from scale 2 can explain degree heterogeneity. Simple growth models (e.g., preferential attachments models in which nodes are connected to other nodes when they have a similar or higher degree) can explain the existence of hubs in networks (and also assortativity, see: Barabasi and Albert, 1999; Newman, 2002). These networks are highly resilient against random attacks and might have optimized evolutionary constraints for robustness (Achard et al., 2006; Albert et al., 2000). However, while clustering can still exist in preferential attachments models, it is dependent on graph size and can therefore not explain clustering as measured in brain networks.

Scale 3 represents the higher-order organization of networks that facilitates functional adaptability. Ravasz and Barabasi (2003) proposed that hierarchical modular networks can combine clustering and the existence of hubs into 1 model. Importantly, hierarchical modular topologies allow for functional degeneracy, representing an evolutionary solution that optimizes functional adaptability (i.e., different combinations of neurons can achieve similar functional output, e.g., Price and Friston, 2002; Tononi et al., 1999). However, in contrast to the models of the first 2 scales a simple universal model to explain hierarchical modular networks has yet to be developed.

Table 2
Details of networks studied in AD

Study	Modality	Network size (template)	Connectivity measure	Weighted or binary	Sparsity level explored	Properties studied	Hubs assessed	Additional comments
1. Stam et al., 2007	EEG	21	SL	Binary	15%	K, C, L, C_{random}, L_{random}, γ, λ, σ	na	Only beta band studied
2. de Haan et al., 2009	EEG	21	SL	Binary	25%	C, L, A, γ, λ, σ	na	In each frequency band studied
3. Stam et al., 2009	MEG	149	PLI	Weighted	nr	C_w, L_w, γ_w, λ_w, σ_w	na	Targeted attack modeling with hubs
4. de Haan et al., 2012c	MEG	149	SL	Weighted	nr	modularity	Yes, threshold not reported	All frequency bands studied
5. Supekar et al., 2008	fMRI	90 (AAL)	Correlation	Binary	nr	C, L, γ, λ, σ, E_{global}	na	For each wavelet
6. Sanz-Arigita et al., 2010	fMRI	90 (AAL)	SL	Binary	K = 5–15	K, C, L, C_{random}, L_{random}, γ, λ, σ	na	Three different templates to define nodes
7. Lo et al., 2010	DTI	78 (AAL)	White matter tracts	Weighted (with FA and number of tracts found)	nr	C_w, L_w, γ_w, λ_w, σ_w, E_{global_w}, E_{local_w},	E_{nodal} > mean (E_{nodal}) + SD (E_{nodal})	—
8. He et al., 2008	sMRI	54 (ANIMAL)	Cortical thickness correlations	Binary	6%–40%	C, L, γ, λ, σ, BC	Standardized BC > 1.5	Targeted attack
9. Yao et al., 2010	sMRI	90 (AAL)	Cortical volume correlations	Binary	15%–30%	K, C, L, C_{random}, L_{random}, γ, λ, σ, BC	Standardized BC > 2 (sparsity level 15%)	—
10. Li et al., 2012	sMRI	90 (AAL)	Cortical thickness correlations	Binary	nr	C	na	Use features for classification
11. Tijms et al., 2013	sMRI	8683 ± 545	Intracortical similarity	Binary	15 ± 0.74%	K, C, L, γ, λ, σ, BC	Standardized BC > 1	—

Key: γ, normalized clustering coefficient; λ, is normalized shortest path length; σ, small-world coefficient (i.e., γ/λ); A, assortativity; AAL is Automated Anatomic Atlas (Tzourio-Mazoyer et al., 2002); AD, Alzheimer's disease; ANIMAL, automated nonlinear image matching and anatomical labeling (Collins et al., 1995); BC, betweenness centrality; C, clustering coefficient; C_{random}, normalized clustering coefficient; DTI, diffusion tensor imaging; EEG, electroencephalography; E_{global}, global network efficiency; E_{local}, local network efficiency; FA, fractional anisotropy; fMRI, functional magnetic resonance imaging; K, degree; L, path length; L_{random}, normalised characteristic path length; MEG, magnetoencephalography; na, not assessed; nr, not reported; PLI, phase lag index; SL, synchronization likelihood; sMRI, structural magnetic resonance imaging; $_w$, weighted variant of metric.

Although these models explain and describe important properties of brain graphs, none of them predict what happens when connections are not only rewired but also lost, which is characteristic for a dysconnectivity disease such as AD. Furthermore, while it can be shown how structure determines functional dynamics, the reverse (inferring structure from function) is more difficult (Honey and Sporns, 2008; Honey et al., 2007, 2010). For these reasons, most graph research in AD has been descriptive. To identify which models can best explain AD, we aim to study which graph properties have been consistently reported to be disrupted within the framework of a heuristic model of graph space.

3. Network disruptions in AD

Table 4 and Figs. 2 and 3 show results that have been reported in a total of 13 studies that compared graph properties between AD and control networks, using EEG, MEG, fMRI, DTI, and sMRI data. It can be seen in Table 2 that most studies investigated only properties that are from scale 1 in the model of Fig. 1, which are related to the balance of information integration and segregation. Four studies also included hubs, which contain information about scale 2. Just 1 study has investigated scale 3 in AD. In this section we will discuss the findings from these studies in more detail.

3.1. Graph connectivity changes in AD

Four studies found a global decrease of functional connectivity (Stam et al., 2009; 2007; Supekar et al., 2008; Zhao et al., 2012). However, Supekar et al. (2008) also found global increased connectivity depending on the frequency band investigated. Two studies did not find group differences in global connectivity (Sanz-Arigita et al., 2010; Tijms et al., 2013). The other 4 studies did not report whether global connectivity was different between AD and control networks (Table 4).

At the local level of the nodes, 4 studies reported connections that were significantly different between groups after correction for multiple comparisons (He et al., 2008; Stam et al., 2007, 2009; Yao et al., 2010). Fig. 2 summarizes connectivity changes in AD for the 4 major cortical lobes (frontal, parietal, temporal, and occipital), because the studies used different anatomical resolutions (ranging from 21 to 90 nodes). This figure shows that in AD connections were mostly affected between lobes, apart from the right temporal lobe that also showed within-lobe connectivity disruptions.

Furthermore, decreases and increases of connectivity strength were found. Though decreased connectivity might be a direct consequence of corticocortical dysconnectivity, increased connectivity is more difficult to interpret. Increases could reflect compensatory mechanisms; however, the relationship between compensatory mechanisms and graph alterations has not yet been thoroughly investigated.

3.2. The average characteristic path length in AD

Table 4 shows that the unnormalized path length was most consistently reported by 6 of 8 studies to be increased in AD. Increased path length has been interpreted to result from the loss connectivity. However, normalized path lengths (i.e., divided by the average path length of random reference graphs) were less consistent across studies: 3 studies (EEG, fMRI, and DTI) also found an increased normalized path length, suggesting that the network moves away from a random network. In contrast, 4 other studies (EEG, MEG, fMRI, and sMRI) reported a decreased normalized path length, suggesting that in AD the network becomes more random.

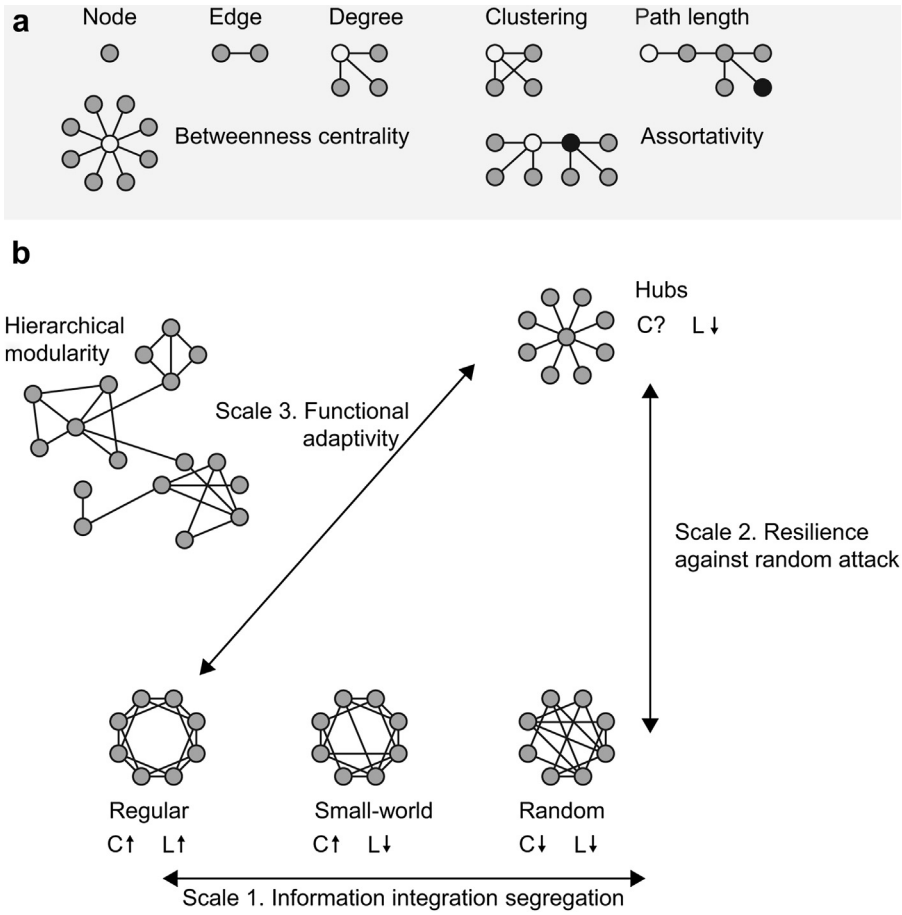

Fig. 1. (a) Depicts the graph properties discussed in this review. The basic building blocks of graphs are nodes and the connecting edges. The degree is simply the number of edges originating from a node: the degree for the white node is 3. The clustering coefficient measures how well neighbors of a given node are connected. The clustering coefficient for the white node is 1/3 (the maximum possible number of connections is 3, of which 1 exists). The shortest path length between the white and the black node is 3. The betweenness centrality for the white node is maximal, because all shortest paths run through this node. When this node is removed, the graph will become completely disconnected. Finally, assortativity is the correlation of the degrees of 2 neighboring nodes. For the white and the black node this is a perfect correlation of 1. (b) This figure illustrates a heuristically defined graph space. The bottom horizontal axes represent scale 1 (i.e., the information integration–segregation scale), shown in the left corner regularly connected networks (i.e., maximal information segregation), intermediate, small-world networks, and in the right corner, randomly connected networks (maximal information integration). The right axis represents scale 2 (i.e., resilience against attack scale), which can explain the existence of hubs. Random networks show low degree heterogeneity and link this axis to scale 1. The star graph at the top of scale 2 is an extreme example of hub models. Other models that fall in this category are scale-free networks, that can be placed more intermediately at this axis. The diagonal axis represents scale 3 (i.e., functional adaptability scale) that combines properties from scale 1 and scale 2. It has been hypothesized that brain graphs have evolved toward modular networks under multiple conflicting constraints. Adopted from Stam and van Straaten (2012) and Solé and Valverde (2004). Abbreviations: C, clustering coefficient; L, path length.

One fMRI study did not find a significant difference in normalized path length between AD and control subjects. This variability in normalized path length suggests that the interpretation of unnormalized path length is ambiguous; Tijms et al. (2013) demonstrated that increased unnormalized path length can be associated with a decreased normalized path length when nodes become disconnected.

Measurements of path length have been associated with disease severity as measured by the Mini Mental State Examination (MMSE; Folstein et al., 1975). In EEG shorter unnormalized path lengths were related to better cognitive functioning (Stam et al., 2007). Similarly, in MEG normalized path length showed a positive correlation with MMSE, suggesting that longer path lengths were related to more cognitive impairment (de Haan et al., 2009). The DTI study found a negative relationship of path length and disease severity in the right middle orbitofrontal gyrus, and several other associations with more specific neuropsychological tests (Lo et al., 2010). One sMRI study found that shorter normalized path length was related to decreased MMSE, suggesting that worse cognitive functioning was associated with a more random graph topology (Tijms et al., 2013). Two other studies failed to find a relationship between MMSE and normalized path length in AD (Sanz-Arigita et al., 2010; Stam et al., 2009).

3.3. The clustering coefficient in AD

Of the 8 studies that investigated the average clustering coefficient, 3 studies did not find differences between AD and control subjects, 2 studies found a decrease in AD, and 3 studies found an increased clustering in AD (see Table 4). In addition to the studies reported in Table 2, another sMRI study assessed differences between groups in the change of clustering over time, which decreased at a rate that was similar for AD and control groups (Li et al., 2012).

Studies that did not find differences between AD and control subjects in clustering also failed to find differences in the normalized clustering coefficient. Four studies reported a decreased normalized clustering coefficient (2 of these did not report the unnormalized clustering coefficient).

All studies reported that networks in AD and control subjects were small-world, suggesting a significantly different topology

Table 3
Explanation of graph theoretical properties that have been studied in Alzheimer's disease

Property	Node definition	Whole network definition
Node: building block of a graph. Also called vertex. The size of a graph is equal to the total number of vertices, V	v_i	$V = \sum_i v_i$
Degree: the number of connections a node has. a_{ij} and w_ij are respectively the binary and weighted values of the cells in the adjacency matrix that indicate the connection status between node pairs i and j		
Binary:	$k_i = \sum_{j \in V} a_{ij}$	$\overline{k} = \frac{1}{V}\sum_{i \in V} k_i$
Binary:	$k_i^w = \sum_{j \in V} w_{ij}$	$\overline{k}^w = \frac{1}{V}\sum_{i \in V} k_i^w$
Connectivity density/sparsity/cost: the ratio of the sum of k to the maximum value of k ($V(V-1)$)	—	$S = \frac{\sum_{i \in V} k_i}{V(V-1)}$
Path length: the minimum number of edges between node pairs i and j		
Binary (Stam et al., 2007; Supekar et al., 2008; Watts and Strogatz, 1998*; Yao et al., 2010)	$L_i = \frac{\sum_{j \neq i \in V} L_{ij}}{(V-1)}$	$L = \frac{\sum_{i \in V} L_i}{V}$
Binary/weighted: harmonic mean (de Haan et al., 2009; He et al., 2008; Newman, 2003*; Sanz-Arigita et al., 2010)	—	$L = \frac{1}{V\left(\sum_{i \in V} \frac{1}{L_i}\right)}$
Weighted (Lo et al., 2010; Stam et al., 2009) (note that the weight w_{ij} might be inversed or not depending on the modality used)	$L_i^w = \frac{\sum_{i \neq i \in V} \frac{1}{W_{ij}}}{(V-1)}$	-
Global efficiency: inverse of the shortest path lengths		
Latora and Marchiori, 2001*; Supekar et al., 2008	—	$E_{Global} = \frac{1}{V(V-1)}\sum_{i \in V} \frac{1}{L_i}$
Nodal efficiency: the average of the inverse of the number of edges between node i and all other nodes in the network		
Weighted (Achard and Bullmore, 2007*; Lo et al., 2010)	$E_{nodal_i} = \frac{1}{(V-1)}\sum_{j \neq i \in V} V \frac{1}{L^w(i,j)}$	—
Clustering ratio of the number of edges between the direct neighbours of node i, indicated by subgraph g_i to the total number of possible edges		
Binary (de Haan et al., 2009; He et al., 2008; Luce and Perry, 1949*; Sanz-Arigita et al., 2010; Stam et al., 2007; Supekar et al., 2008; Yao et al., 2010)	$c_i = \frac{\sum_{k_j \in g_i} k_j}{k_{g_i}(k_{g_i}-1)/2}$	$C = \frac{\sum_{i \in V} C_i}{V}$
Weighted: ratio of the weights of the neighbors of node i (Stam et al., 2009*)	$c_i^w = \frac{\sum_{k \neq j}\sum_{j \neq i,k} w_{ij} w_{ik} w_{jk}}{\sum_{k \neq i}\sum_{i \neq i,k} w_{ik} w_{ij}}$	$C = \frac{\sum_{i \in V} C_i^w}{V}$
Weighted: similar to above, with weights scaled by the mean weight of all weights (Lo et al., 2010; Onnela et al., 2005*)	$c_i^w = \frac{2}{k_i(k_i-1)}\sum_{j,k \in V} (\overline{w}_{ij}\overline{w}_{jk}\overline{w}_{ik})^{1/3}$	$C = \frac{\sum_{i \in V} C_i^w}{V}$
Local efficiency: Similar interpretation as clustering coefficient, G_i denotes subgraph of graph G (Latora and Marchiori, 2001*; Lo et al., 2010)		
	—	$E_{Local} = \frac{1}{V}\sum_{i \in G} E(G_i)$
Assortativity: the correlation between the degrees of all pairs of nodes. K is the number of edges, jl_i and k_{mi} are the degrees of nodes connected by edge i		
Newman, 2002*; Stam et al., 2007	—	$r = \frac{\frac{1}{K}\sum_{i \in K} l_i, m_i - \left(\frac{1}{K}\sum_{i \in K}\frac{1}{2}(l_i + m_i)\right)^2}{\frac{1}{K}\sum_{i \in K}\frac{1}{2}(l_i^2 + m_i^2) - \left(\frac{1}{K}\sum_{i \in K}\frac{1}{2}(l_i + k_i)\right)^2}$
Normalization procedures: to determine the small-world coefficient, average clustering and average path lengths are normalized by the value of null model networks. Regular: Sanz-Arigita et al. (2010); Stam et al. (2007); random: Sanz-Arigita et al. (2010); Stam et al. (2007); random with degree intact: de Haan et al. (2009); Maslov and Sneppen (2002)*; Sanz-Arigita et al. (2010); Stam et al. (2007); Supekar et al. (2008); random with weight distribution intact: Stam et al. (2009)	$\widehat{L}_i, \widehat{C}_i$	$\widehat{L}, \widehat{C}$
Small world: a network is 'small-world' when the clustering coefficient is higher than a random network, and when the path length is approximately equal to a random network		
	—	$\sigma = \frac{C/\widehat{C}}{L/\widehat{L}}$
Betweenness centrality: the proportion of shortest paths S between node j and m that run through a node i (Freeman, 1977*; He et al., 2008; Yao et al., 2010)	$BC_i = \sum_{i \neq j \neq m \in V} \frac{S_{j,m}(i)}{S_{j,m}}$	$BC = \frac{1}{V}\sum_{i \in V} BC_i$
Modularity: indicates whether a graph can be divided into subgraphs that show high intraconnectivity and low interconnectivity. Here m is the number of modules, l_s is the sum of weights in module s, L is the total sum of all weights in the network and d_s is the sum of the strength of all vertices in module s (de Haan et al., 2012a; Stam, 2010*)	—	$Q_m^w = \sum_{s \in m} \frac{l_s}{L} - \left(\frac{d_s}{2L}\right)^2$
Within module degree: measures the degree within a module. The weights between node i and other nodes in the module, normalized by the average module weight and standard deviation		
de Haan et al., 2012a; Guimera and Amaral, 2005*	$z_i^w = \frac{k_i^w(m_i) - \overline{k}^w(m_i)}{\sigma^{k^w}(m_i)}$	—
Participation coefficient: measures how strongly a node i is connected to other modules m in the set of modules M. A provincial hub as a high within-module degree and low participation coefficient. A connector hub has a high participation coefficient and a low within-module degree		
de Haan et al., 2012a; Guimera and Amaral, 2005*	$PC_i^w = 1 - \sum_{m \in M}\left(\frac{k^w(m)}{k_i^w}\right)^2$	—

Cells marked with '—' indicates this measurement has not been assessed and will therefore not be discussed.
Key: * is study from which the graph property definition was obtained.

Table 4
Comparison of graph theoretical properties of graph studies and AD

Property	AD > H	AD < H	NS	NR
gc	Supekar et al., 2008	Stam et al., 2007, 2009; Supekar et al., 2008; Zhao et al., 2012	Sanz-Arigita et al., 2010; Tijms et al., 2013	de Haan et al., 2009; He et al., 2008; Lo et al., 2010; Yao et al., 2010
L	He et al., 2008; Lo et al., 2010 [a]; Stam et al., 2007 [c], 2009 [a]; Yao et al., 2010; Zhao et al., 2012	Sanz-Arigita et al., 2010; Tijms et al., 2013	—	de Haan et al., 2009; Supekar et al., 2008
C	He et al., 2008; Yao et al., 2010; Zhao et al., 2012	Stam et al., 2009 [a,b]; Tijms et al., 2013	Lo et al., 2010 [a]; Sanz-Arigita et al., 2010; Stam et al., 2007	de Haan et al., 2009; Supekar et al., 2008
λ	Lo et al., 2010 [a,b]; Stam et al., 2007 [b]; Zhao et al., 2012	de Haan et al., 2009 [b,d]; Sanz-Arigita et al., 2010; Stam et al., 2009 [a,b]; Tijms et al., 2013	Supekar et al., 2008	He et al., 2008; Yao et al., 2010
γ	Zhao et al., 2012	de Haan et al., 2009[b]; Stam et al., 2009[a,b]; Supekar et al., 2008; Tijms et al., 2013	Lo et al., 2010[a,b]; Sanz-Arigita et al., 2010	He et al., 2008; Yao et al., 2010
σ	Zhao et al., 2012	de Haan et al., 2009[b]; Supekar et al., 2008; Tijms et al., 2013	Lo et al., 2010[a]	He et al., 2008; Sanz-Arigita et al., 2010; Stam et al., 2007, 2009; Yao et al., 2010

Key: γ, average normalized clustering coefficient; λ, average normalized characteristic path length; σ, small-world property (= γ/λ); AD, Alzheimer's disease; C, clustering coefficient; gc, global connectivity; H, control group; L, average characteristic path length; NR, not reported; NS, not significant.

[a] Weighted.
[b] Alpha band.
[c] Beta band.
[d] Gamma band.

from that of random networks. Three studies reported a decreased (i.e., more random) small-world value in AD, and 1 study failed to find such a difference.

It remains unclear from these studies whether networks in AD become more random or regular at scale 1. Possibly the clustering coefficient is less affected by AD, while the path length increases. Such a situation could arise when higher-level graph properties of a network (e.g., modularity), are altered.

3.4. Modularity in AD

de Haan et al. (2012c) found fewer modules in AD than in control subject MEG networks. This difference was significant in the theta, beta, and gamma frequency bands, although with different topologies.

In the beta and gamma band the value of the modularity metric was decreased in AD. Only in the beta band a decreased intramodular connectivity was found, while the intermodular connectivity was similar to that in control networks. The decreased connectivity was specific for the parietal cortex, suggesting a loss of provincial hubs.

In contrast, the modularity value in the theta band was increased in AD. Intermodular connectivity was decreased, and intramodular connectivity did not differ between AD and control groups, suggesting a loss of connector hubs. The findings in the theta band are most in line with a relatively intact local clustering and an increased path length as found in networks from different imaging modalities.

3.5. Hubs in AD

The previous sections suggest that hubs in networks might be selectively vulnerable in AD (first proposed by Buckner et al., 2005, 2009). Only 3 studies explicitly reported spatial patterns of hubs in AD (see Table 2), and therefore we also included studies that investigated hubs in healthy aging (Meunier et al., 2009; Wang et al., 2010; Zhu et al., 2012). Most of these studies identified hubs as nodes with normalized betweenness centrality values 1.5 times higher than average (He et al., 2008; Lo et al., 2010; Wang et al., 2010; Yao et al., 2010; Zhu et al., 2012), apart from Meunier et al. (2009) who defined hubs as nodes that had a higher than average degree within a module. All but 1 study investigated networks with 90 nodes corresponding to the AAL atlas (He et al., 2008 used 54 anatomical areas). Four studies assessed hubs in a connectivity density range of 13% to 15% (He et al., 2008; Lo et al., 2010; Wang et al., 2010; Yao et al., 2010), and 2 studies compared hubs in sparser networks of 5% (Meunier et al., 2009) and 6.1% (Zhu et al., 2012).

Fig. 3 gives an overview of the hubs that were found by these studies (see Table 5 for abbreviations of the anatomical areas). Here we focus on the hubs that were reported by more than 2 studies, suggesting a more stable finding.

Strikingly, in AD only 7 hubs were identified; less than half of the 16 hubs that were reported in control subjects. The loss of hubs in AD might be explained by atrophy of particular areas, because these areas are known to be lesioned (e.g., temporal regions, insula, cingulate, and parietal regions). Using a spectral graph approach, de Haan et al. (2012b) found that decreases of local centrality were related to worse cognitive decline. Tijms et al. (2013) reported decreased betweenness centrality in the posterior cingulate and medial temporal structures that is also suggestive of a loss of hubs.

It remains unclear whether hubs that appeared to be stable, were robust against AD or were still affected by the disease. Although these areas lost connections, some important shortcuts

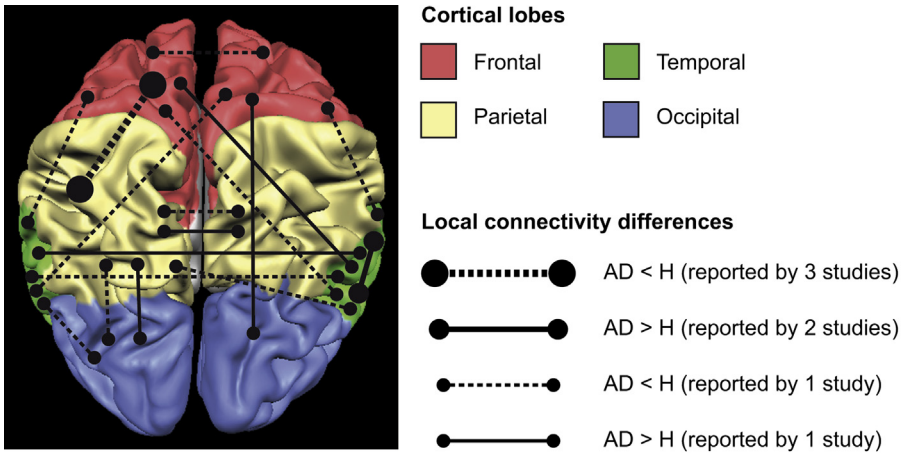

Fig. 2. Visualization, in neurological convention, of differences in local connectivity as reported by Stam et al. (2007) (EEG), He et al. (2008) (sMRI), Yao et al. (2010) (sMRI), and Stam et al. (2009) (MEG, reported in 8–10 Hz and 13–30 Hz). Because of differences in anatomical templates and/or reference points, the connectivity is summarized over the 4 major lobes. Abbreviations: AD, Alzheimer's disease patient group; H, control group.

might still run through these nodes (also see: de Haan et al., 2012c). Alternatively, these areas become relatively more important when other hubs degrade.

Interestingly, de Haan et al. (2009) reported decreased assortativity (i.e., degree correlation) in the alpha band of AD networks in comparison with controls. It has recently been reported that hubs in DTI graphs tend to be strongly interconnected, forming a 'rich club' (van den Heuvel and Sporns, 2011; van den Heuvel et al., 2012). The decreased assortativity in AD suggests that the connectivity among hubs is damaged.

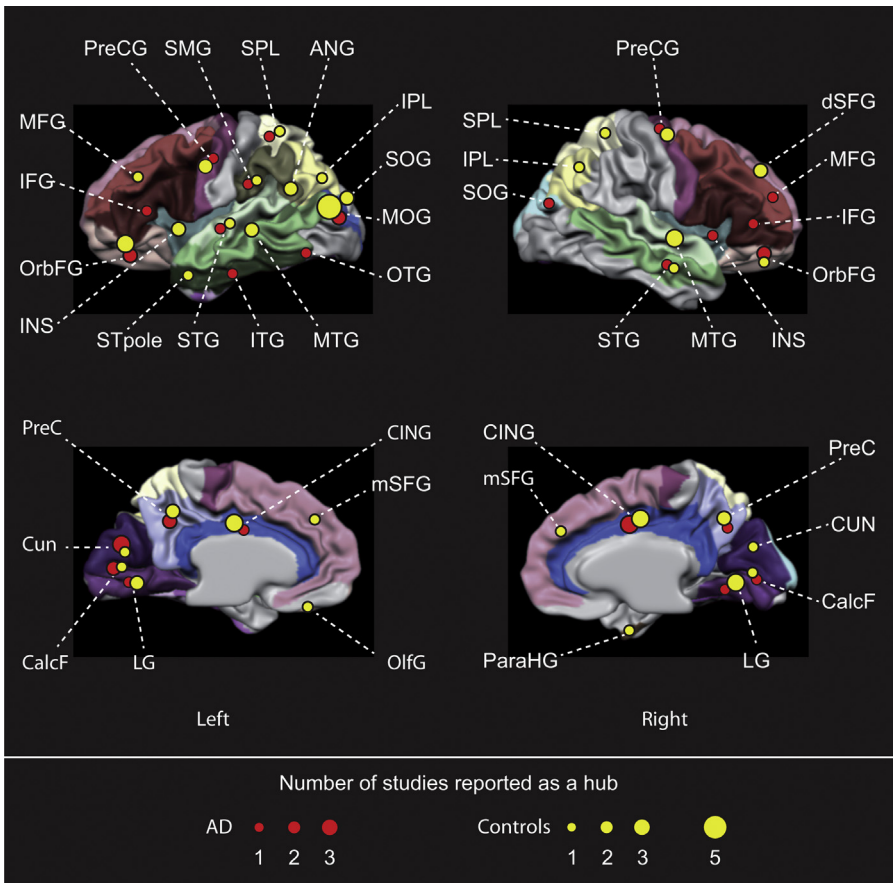

Fig. 3. Visual overview of anatomical locations found to have a hub role in AD (red circles) and control (yellow circles) subjects. Different colors for cortical areas correspond to different major gyri (and 1 sulcus), at a coarser resolution than AAL because 1 study used a lower resolution (54 anatomical regions, He et al., 2008). Circle diameter is proportional to the number of studies that reported the region to be a hub. When circles overlap the studies reported the same cortical region, when circles do not overlap, different regions within this area were reported. In total, 19 unique areas were identified as a hub by more than 2 studies. Section 2 of the Supplementary data includes a list of the studies that reported these regions. See Table 5 for a list of anatomical areas and their abbreviations. Abbreviations: AAL, automated anatomical labeling atlas; AD, Alzheimer's disease.

Table 5
Anatomical areas and their abbreviations

Abbreviation	Anatomical area
ANG	Angular gyrus
CalcF	Calcarine fissure
CING	Cingulate gyrus
CUN	Cuneus
dSFG	Dorsal superior frontal gyrus
IFG	Inferior frontal gyrus
INS	Insula
IPL	Inferior parietal lobule
ITG	Inferior temporal gyrus
LG	Lingual gyrus
MFG	Middle frontal gyrus
MOG	Middle occipital gyrus
mSFG	Medial superior frontal gyrus
MTG	Middle temporal gyrus
OlfG	Olfactory gyrus
OrbFG	Orbitofrontal gyrus
OTG	Occipitotemporal gyrus
ParaHG	Parahippocampal gyrus
PreC	Precuneus
PreCG	Precentral gyrus
SMG	Supramarginal gyrus
SOG	Superior occipital gyrus
SPL	Superior parietal lobule
STG	Superior temporal gyrus
STpole	Superior temporal pole

Two studies further investigated how the removal of hub nodes or hub connections influences other network properties. He et al. (2008) scrutinized sMRI networks in AD and healthy aging samples by removing nodes either randomly or by specifically targeting the hubs. Network robustness was measured as the relative size of the largest component (i.e., graph without isolated nodes). When random nodes were removed, AD and control networks were similarly affected. However, AD networks reduced faster in size than the control networks when hubs were cut, suggesting that the topology of AD networks are more vulnerable to future attacks.

Using MEG networks, Stam et al. (2009) used a different approach to investigate the effects of random and targeted attacks to networks. They damaged a healthy subject's network by weakening the edges until the global connectivity level resembled that of an empirically derived AD network, and then assessed whether the network properties of the damaged network were comparable with those of an AD network. They found that when hubs were selectively targeted, the clustering coefficient decreased, also supporting a selective vulnerability of hubs in AD.

4. Discussion

4.1. Summary and interpretation of graph disturbances in AD

This study investigated which graph properties were most consistently reported to be disrupted in AD, and into which direction AD topology changes in a heuristically defined graph space. In AD, decreases and increases in the number of functional and structural relationships were observed, suggesting a loss and reorganization of connectivity. In addition, most disrupted connections spanned across cortical lobes, indicating a specific vulnerability of long-range connections (note however that the spatial resolution of EEG only detects long-range connectivity). Most of the reviewed studies investigated only scale 1 in graph space. Table 4 shows that for this scale there is as much evidence for random as for more regular network topologies, regardless of the imaging modality used. The divergent findings across studies suggest that although scale 1 has been investigated in most studies, it might not be the best scale to investigate network properties in AD. More consistent disruptions in AD were an increased average unnormalized path length across all imaging modalities and a decreased number of hubs in sMRI and DTI graphs. Although this might support the isometric nature of brain graphs, the interpretation of increased unnormalized path lengths remains ambiguous, because considerable variability exists across studies in normalized path length differences.

Average (normalized) path length was correlated with disease severity in 2 studies, however, 3 other studies failed to find such a relationship. Although differences in spatial hub patterns have only been studied in anatomically defined networks, these results are in line with a functional study that demonstrated a decreased modularity in AD. Evidence from these studies suggests that AD brain graphs become more random because of the loss of modularity and degree heterogeneity.

Interestingly, hubs that were reported in control but not in AD graphs corresponded to the regions that typically show AD pathology. These associative regions in the temporal, parietal, and frontal cortices link other cortical areas with long-range cortico-cortical connections, playing an important role in sensory integration (e.g., Arnold et al., 1991; Delbeuck et al., 2003; Pearson et al., 1985). Losing connectivity in these areas might have caused the increase in average path length across studies.

Recently, associations between spatial AD pathology patterns (e.g., amyloid deposition measured with positron emission tomography) and functional disruptions have been reported in healthy (young) individuals, suggesting that AD pathology is related to the levels of activation in hub regions (Buckner et al., 2009; Sperling et al., 2009; also see: Jagust and Mormino, 2011). Transgenetic mice studies have found a causal and positive relationship between cellular activity and amyloid deposition further supporting this "activity causes damage" hypothesis (Bero et al., 2011; Cirrito et al., 2005). Interestingly, cortical areas that lose functional connectivity have been related to cortical atrophy (e.g., Seeley et al., 2009), which suggests that "neurons that wire together die together" (Sepulcre et al., 2012).

4.2. Alternative explanations of graph disturbances in AD

4.2.1. Differences between imaging modalities and graph construction methods

Diverging results might imply that brain graphs are not isomorphic across imaging modalities and instead measure different aspects of brain graphs reflecting specific spatial and temporal resolutions. For example, the network derived at the micro level of neurons in *C. elegans* shows negative assortativity (Newman, 2002); and human brain graphs measured at the macro level show positive assortativity (e.g., Bassett et al., 2008; de Haan et al., 2009). However, findings diverged even within imaging modalities, suggesting that other confounding factors are likely to be involved.

A possible confounder is the lack of a standardized method to construct graphs. It has been demonstrated that the size and connectivity density influence the values of other graph properties and should therefore be kept constant when comparing graphs (see e.g., Fornito et al., 2010; van Wijk et al., 2010; Zalesky et al., 2010). The studies in this review were all of different size, ranging from 21 in EEG to 8683 $\pm$ 545 nodes in sMRI. The interpretation of graph properties is further complicated by the fact that nodes represent different amounts of cortical tissue, causing differences in signal to noise ratios (but see: Hillebrand et al., 2012). Mapping nodes between different graphs is not a trivial task. Anatomical atlases can

serve as reference points and usually have a clear histological definition. However, subjects show great variability in their gyri and sulci patterns, complicating accurate mapping of atlases between individuals. In addition, although atlas-based cortical areas might still be defined in AD, the influence of local atrophy on nodal properties has not yet been thoroughly investigated. Template-free methods such as voxelwise approaches also exist, and should be further explored in AD (e.g., Buckner et al., 2009; Hagmann et al., 2007; Tijms et al., 2012; van den Heuvel et al., 2008), although template-free approaches might reintroduce the problem of differently sized graphs across individuals (Tijms et al., 2013).

Differences in the definition of the connectivity function might explain why an increased clustering coefficient was found in group-based sMRI, and most functional studies found a decrease. An increased clustering coefficient might simply reflect atrophy processes that introduce more similarity of cortical morphology in AD patients. Alternatively, the decreased number of hubs contributed to an increased clustering coefficient: hubs usually display low clustering, because they connect many nodes that would otherwise not be connected.

Combining information from multiple imaging modalities is in general a difficult issue. Recently computational simulation models have been used to further scrutinize the relationship between different types of connectivity. For example, it has been shown that functional connectivity can arise between cortical areas that are not directly connected with DTI traced tracts (e.g., Honey et al., 2007, 2009). Similarly, only 60% of positive correlations in cortical thickness converged with DTI traced tracts (Gong et al., 2012). The relationship between functional and structural graphs remains an open question, which is complicated by the fact that covariation between cortical areas across individuals might capture different regularities than connectivity functions defined within a subject. New methods exist to describe single-subject gray matter graphs that do allow for direct mapping between graphs from other modalities (e.g., Tijms et al., 2012).

Within functional studies, nonlinear versus linear methods to assess connectivity might have caused diverging results. Additionally, recent studies have shown that spurious functional connectivity can arise from head movement during scanning despite correcting for this during preprocessing (Power et al., 2012; van Dijk et al., 2012). Furthermore, it would be interesting to investigate how graph properties fluctuate over time, because evidence has been reported that the functional modular architecture of the brain is nonstationary and that this differs between patients and control subjects (see e.g., Jones et al., 2012).

Estimation reliability seems an unlikely confounder, because recent studies have demonstrated that graph properties show moderate to strong reliability when measured at 2 time points within the same sample in DTI (Bassett et al., 2011; Vaessen et al., 2010), MEG (Deuker et al., 2009), fMRI (Telesford et al., 2010; Wang et al., 2011), and sMRI (Tijms et al., 2012) studies.

Finally, differences in global connectivity between AD and control networks are likely to introduce differences in the number of weak connections included and the number of disconnected nodes. Although weighted network measurements eliminate the need for arbitrary thresholds, they remain sensitive for such a priori existing weight differences (also see: Toppi et al., 2012). Minimum spanning trees provide an alternative approach to investigate network topologies. A minimum spanning tree connects all nodes in a graph at a minimum cost (defined as 1 - the weight of an edge) and might be considered as the connectivity backbone of a graph, ensuring that all graphs have the same amount of edges. Çiftçi (2011) has used this tool to compare minimum spanning trees between AD and control groups based on resting state connectivity of 36 default mode network areas. Importantly, the degree distribution was similar between groups, and the AD group was characterized by higher segregation in the network than in the control group. Future research should further investigate this at a whole brain level and in different imaging modalities.

4.2.2. The influence of sample composition

The presently reviewed studies differed in the composition of AD patient samples, which probably also contributed to the variability in reported findings. The characterization of AD might not be as straightforward as the classical description suggests. Subtypes of AD have been described, characterized by different atrophy patterns than in the medial temporal lobes and where memory loss is not a prominent feature. For example, 1 subtype of AD develops typically at younger ages (i.e., early-onset AD, younger than 65 years) and is characterized by a posterior cortical atrophy pattern that is accompanied by visuoperceptual problems (e.g., Benson et al., 1988; Crutch et al., 2012; Frisoni et al., 2005; Karas et al., 2007; Lehmann et al., 2012; Ridgway et al., 2012; Smits et al., 2012; van der Flier et al., 2011). Different spatial patterns of pathological markers such as cortical atrophy, plaques, and tangles will influence network topologies, as has been reported in frontotemporal dementia (de Haan et al., 2009; also see Zhou et al., 2010).

The divergent results across studies possibly reflect the heterogeneity of AD, because the age ranges reported across the studies (between 51 and 90 years) are likely to include patients with early-onset AD. In addition, healthy aging also affects graph properties (Achard and Bullmore, 2007; Chen et al., 2011; Gong et al., 2009b; Meunier et al., 2009; Wen et al., 2011; Zhu et al., 2012). Some studies included people with subjective memory complaints that might be very early manifestations of the disease, and other studies included cognitively healthy people without memory complaints.

The presence of apolipoprotein E (APOE) gene with allelic variant 4 (APOE4) increases the risk to develop AD, and has been associated with disturbed functional connectivity in cognitively healthy people (e.g., Damoiseaux et al., 2012; Filippini et al., 2009, 2011; Sheline et al., 2010) and with disrupted graph topologies in AD (Zhao et al., 2012). Interestingly, the spatial pattern of APOE4-related disturbances overlaps with regions that are vulnerable for AD pathology. Brown et al. (2011) recently demonstrated in healthy APOE4 carriers that aging was associated with reduced clustering in DTI graphs, and that this was specific for the precuneus and cingulate regions. APOE effects might be nonlinear, because Trachtenberg et al. (2012) showed similar disturbances in healthy carriers of the APOE allelic variant 2 that is protective against AD. Different distributions of APOE carriers in subject samples across studies might have contributed to the diverging results across studies reviewed here, and this should be further investigated.

Finally, disease severity measured with the MMSE ranged from as low as 15 to as high as 24, suggestion that disease severity in the patient groups was also heterogeneous.

4.3. Future perspectives

The application of graph theory to investigate network disruptions in AD is still in its early days, and many important open questions remain. Up to now, graph theory has mainly been used to describe networks in AD. An important next step is the formulation of a hypothesis-generating framework to understand how altered network topologies are related to cognitive dysfunctioning.

At this point the models described in the heuristically defined graph space are developmental models: they predict what happens when connections are added or rewired; they do not necessarily predict what happens when connections are removed. A heuristic model of graph space is an important first step toward defining

a more elegant model to generate hypotheses predicting what happens to networks when connections are not only rewired, but also lost. Furthermore, graph theory might also be used as a clinical tool.

4.3.1. Practical applications of graph theory

The potential of graph properties for early diagnosis of AD has been investigated in people who were diagnosed with minor cognitive impairment (MCI) that has been associated with an increased risk to develop AD (Petersen et al., 1999). Studies that have compared MCI graphs with AD and healthy subjects have suggested that MCI topologies are intermediate (Li et al., 2012; Liu et al., 2012; Yao et al., 2010). Significant, but subtle, differences have been reported when comparing MCI with healthy elderly subjects, suggesting that larger samples are required when comparing 3 groups (Bai et al., 2012; Buldú et al., 2011; Shu et al., 2012; Wang et al., 2012).

The diagnostic potential of graph properties has also been explored and high classification accuracies >80% have been reported (Li et al., 2012; Wang et al., 2012; Wee et al., 2011, 2012; for a review see Horwitz and Rowe, 2011). However, such high classification accuracies can also be obtained with basic connectivity measurements (Dai et al., 2011; Shao et al., 2012; Zhou et al., 2011; for a multimodal approach see: Dai et al., 2012). A general problem when many features are used for classification is the 'curse of dimensionality', meaning that much data is needed to build a classifier that generalizes to unseen cases. Dimensionality reduction by means of feature selection (e.g., by choosing only features that maximize group differences) can still inflate the subsequent performance of the classifier and thereby reduce its generalizability. More research is needed to further investigate the generalizability of these classifiers.

Several studies have found moderate to strong correlations between graph properties and neuropsychological measurements in AD and MCI (de Haan et al., 2009, 2012c; Lo et al., 2010; Sanz-Arigita et al., 2010; Shu et al., 2012; Stam et al., 2007, 2009; Tijms et al., 2013 Wang et al., 2012). This suggests that graph properties have potential to monitor disease progression in AD, which is important for the development of new therapies. Longitudinal studies are necessary to further validate disease-monitoring properties in individual subjects.

4.3.2. Computational modeling of AD and graph theory

The use of computational simulation models is important for the development of a generative model of AD. Computational modeling requires the explicit formulation of processes and can generate hypotheses for further empirical investigations. For example, relating different modalities to each other is a general difficult question for neuroimaging. By combining computational modeling and graph theoretical approaches, Honey et al. (2009) demonstrated how functional connectivity is related to DTI connectivity.

Albert et al. (2000) used simulation modeling to show that scale-free complex networks are robust to random removal of edges and/or nodes, but become disconnected when hubs are targeted. This model suggests that a change of graph topology might be associated with increased vulnerability to random and/or targeted attacks. In empirical data, such hub vulnerability was demonstrated by He et al. (2008) and Stam et al. (2009) (see section 3.5).

Recently, de Haan et al. (2012a) used computational modeling to further investigate whether hub nodes are more vulnerable to activity-dependent degeneration. An important result of this study is a new specific prediction about AD disease mechanisms that can be empirically tested in patient data, and might lead to new therapeutic strategies targeting disturbed neuronal activity.

Network connectivity might also explain how specific atrophy patterns arise: Raj et al. (2012) modeled the disease propagation of different types of dementia (AD and frontotemporal dementia) with a diffusion model. Their main result suggested that different atrophy patterns were related to collections of cortical areas that were connected by specific axonal tracts (also see Seeley et al., 2009). In other words, axonal connectivity determines the spread of disease. Zhou et al. (2012) reached a similar conclusion using resting state fMRI to predict regional vulnerability for atrophy. Although these models need further validation, these studies illustrate how neuroimaging can be pushed forward by a combined graph theoretical and computational modeling approach, which is crucial to gain more insight into complex network diseases such as AD.

4.4. Conclusion

Until the precise mechanism that generates connectivity in brain graphs has been uncovered, descriptive analyses remain important. The diverging findings suggest that brain graphs across imaging modalities are not isometric but instead measure different aspects of brain connectivity. Although this considerably complicates the interpretation of graph measurements, it also suggests that multimodal research is needed to better understand the structure–function relationship of the brain.

In conclusion, the use of graph theory has moved research forward from studying cortical areas in isolation, by identifying why certain regions are more vulnerable based on their role in a network. If we succeed in unifying different imaging modalities, we can have a spatiotemporally detailed view on brain connectivity in health and disease.

Disclosure statement

The authors declare no conflicts of interest.

Acknowledgements

This study was conducted at the VUmc Alzheimer center that is part of the neurodegeneration research program of the Neuroscience Campus Amsterdam. The VUmc Alzheimer center is supported by Alzheimer Nederland and Stichting VUmc fonds. The authors thank the reviewers and Ilse van Straaten for their valuable comments and Marijn Groenewoud for assistance with the figures.

Appendix A. Supplementary data

Supplementary data associated with this article can be found, in the online version, at http://dx.doi.org/10.1016/j.neurobiolaging.2013.02.020.

References

Achard, S., Bullmore, E., 2007. Efficiency and cost of economical brain functional networks. PLoS Comp. Biol. 3, e17.

Achard, S., Salvador, R., Whitcher, B., Suckling, J., Bullmore, E., 2006. A resilient, low-frequency, small-world human brain functional network with highly connected association cortical hubs. J. Neurosci. 26, 63–72.

Albert, R., Jeong, H., Barabási, A., 2000. Error and attack tolerance of complex networks. Nature 406, 378–382.

Arendt, T., 2009. Synaptic degeneration in Alzheimer's disease. Acta Neuropathol. 118, 167–179.

Arnold, S.E., Hyman, B.T., Flory, J., Damasio, A.R., van Hoesen, G.W., 1991. The topographical and neuroanatomical distribution of neurofibrillary tangles and neuritic plaques in the cerebral cortex of patients with Alzheimer's disease. Cereb. Cortex 1, 103–116.

Bai, F., Shu, N., Yuan, Y., Shi, Y., Yu, H., Wu, D., Wang, J., Xia, M., He, Y., Zhang, Z., 2012. Topologically convergent and divergent structural connectivity patterns between patients with remitted geriatric depression and amnestic mild cognitive impairment. J. Neurosci. 32, 4307–4318.

Barabasi, A.L., Albert, R., 1999. Emergence of scaling in random networks. Science 286, 509–512.
Bassett, D., Bullmore, E., 2006. Small-world brain networks. Neuroscientist 12, 512–523.
Bassett, D., Bullmore, E., Verchinski, B., Mattay, V., Weinberger, D., Meyer-Lindenberg, A., 2008. Hierarchical organization of human cortical networks in health and schizophrenia. J. Neurosci. 28, 9239–9248.
Bassett, D.S., Brown, J.A., Deshpande, V., Carlson, J.M., Grafton, S.T., 2011. Conserved and variable architecture of human white matter connectivity. Neuroimage 54, 1262–1279.
Benson, D.F., Davis, R.J., Snyder, B.D., 1988. Posterior cortical atrophy. Arch. Neurol. 45, 789–793.
Bero, A.W., Yan, P., Roh, J.H., Cirrito, J.R., Stewart, F.R., Raichle, M.E., Lee, J.M., Holtzman, D.M., 2011. Neuronal activity regulates the regional vulnerability to amyloid-β deposition. Nat. Neurosci. 14, 750–756.
Blennow, K., Bogdanovic, N., Alafuzoff, I., Ekman, R., Davidsson, P., 1996. Synaptic pathology in Alzheimer's disease: relation to severity of dementia, but not to senile plaques, neurofibrillary tangles, or the ApoE4 allele. J. Neural Transm. 103, 603–618.
Braak, H., Braak, E., 1991. Neuropathological stageing of Alzheimer-related changes. Acta Neuropathol. 82, 239–259.
Brown, J.A., Terashima, K.H., Burggren, A.C., Ercoli, L.M., Miller, K.J., Small, G.W., Bookheimer, S.Y., 2011. Brain network local interconnectivity loss in aging APOE-4 allele carriers. Proc. Natl. Acad. Sci. U. S. A 108, 20760–20765.
Buckner, R., Snyder, A., Shannon, B., LaRossa, G., Sachs, R., Fotenos, A.F., Sheline, Y.I., Klunk, W.E., Mathis, C.A., Morris, J.C., Mintun, M.A., 2005. Molecular, structural, and functional characterization of Alzheimer's disease: evidence for a relationship between default activity, amyloid, and memory. J. Neurosci. 25, 7709–7717.
Buckner, R.L., Sepulcre, J., Talukdar, T., Krienen, F.M., Liu, H., Hedden, T., Andrews-Hanna, J.R., Sperling, R.A., Johnson, K.A., 2009. Cortical hubs revealed by intrinsic functional connectivity: mapping, assessment of stability, and relation to Alzheimer's disease. J. Neurosci. 29, 1860–1873.
Buldú, J.M., Bajo, R., Maestú, F., Castellanos, N., Leyva, I., Gil, P., Sendiña-Nadal, I., Almendral, J.A., Nevado, A., del-Pozo, F., Boccaletti, S., 2011. Reorganization of functional networks in mild cognitive impairment. PLoS One 6, e19584.
Bullmore, E.T., Bassett, D.S., 2011. Construction and interpretation of complex networks derived from human neuroimaging data. Annu. Rev. Clin. Psychology 7, 113–140.
Bullmore, E.T., Sporns, O., 2009. Complex brain networks: graph theoretical analysis of structural and functional systems. Nat. Rev. Neurosci. 10, 186–198.
Bullmore, E., Sporns, O., 2012. The economy of brain network organization. Nat. Rev. Neurosci. 13, 336–349.
Chen, Z.J., He, Y., Rosa-Neto, P., Gong, G., Evans, A.C., 2011. Age-related alterations in the modular organization of structural cortical network by using cortical thickness from MRI. Neuroimage 56, 235–245.
Chklovskii, D.B., 2004. Synaptic connectivity and neuronal morphology: two sides of the same coin. Neuron 43, 609–617.
Çiftçi, K., 2011. Minimum spanning tree reflects the alterations of the default mode network during Alzheimer's disease. Ann. Biomed. Eng. 39, 1493–1504.
Cirrito, J.R., Yamada, K.A., Finn, M.B., Sloviter, R.S., Bales, K.R., May, P.C., Schoepp, D.D., Paul, S.M., Mennerick, S., Holtzman, D.M., 2005. Synaptic activity regulates interstitial fluid amyloid-β levels in vivo. Neuron 48, 913–922.
Collins, D.L., Holmes, C., Peters, T.M., Evans, A., 1995. Automatic 3-D model-based neuroanatomical segmentation. Hum. Brain Mapp. 3, 190–208.
Crutch, S.J., Lehmann, M., Schott, J.M., Rabinovici, G.D., Rossor, M.N., Fox, N.C., 2012. Posterior cortical atrophy. Lancet Neurol. 11, 170–178.
Dai, D., He, H., Vogelstein, J., Hou, Z., 2011. Network-based classification using cortical thickness of AD patients. Mach. Learn. Med. Imaging 7009, 193–200.
Dai, Z., Yan, C., Wang, Z., Wang, J., Xia, M., Li, K., He, Y., 2012. Discriminative analysis of early Alzheimer's disease using multi-modal imaging and multi-level characterization with multi-classifier (M3). Neuroimage 59, 2187–2195.
Damoiseaux, J.S., Seeley, W.W., Zhou, J., Shirer, W.R., Coppola, G., Karydas, A., Rosen, H.J., Miller, B.L., Kramer, J.H., Greicius, M.D., Alzheimer's Disease Neuroimaging Initiative, 2012. Gender modulates the APOE ε4 effect in healthy older adults: convergent evidence from functional brain connectivity and spinal fluid tau levels. J. Neurosci. 32, 8254–8262.
Deco, G., Senden, M., Jirsa, V., 2012. How anatomy shapes dynamics: a semi-analytical study of the brain at rest by a simple spin model. Front. Comput. Neurosci. 6, 68.
de Haan, W., Mott, K., van Straaten, E.C.W., Scheltens, P., Stam, C.J., 2012a. Activity dependent degeneration explains hub vulnerability in Alzheimer's disease. PLoS Comp. Biol. 8, e1002582.
de Haan, W., Pijnenburg, Y.A.L., Strijers, R.L.M., van der Made, Y., van der Flier, W.M., Scheltens, P., Stam, C.J., 2009. Functional neural network analysis in frontotemporal dementia and Alzheimer's disease using EEG and graph theory. BMC Neurosci. 10, 101.
de Haan, W., van der Flier, W., Wang, H., van Mieghem, P., Scheltens, P., Stam, C.J., 2012b. Disruption of functional brain networks in Alzheimer's disease: what can we learn from graph spectral analysis of resting-state MEG? Brain Connect. 2, 45–55.
de Haan, W., van der Flier, W.M., Koene, T., Smits, L.L., Scheltens, P., Stam, C.J., 2012c. Disrupted modular brain dynamics reflect cognitive dysfunction in Alzheimer's disease. Neuroimage 59, 3085–3093.
Delbeuck, X., van der Linden, M., Collette, F., 2003. Alzheimer's disease as a disconnection syndrome? Neuropsychol. Rev. 13, 79–92.
Deuker, L., Bullmore, E., Smith, M., Christensen, S., Nathan, P.J., Rockstroh, B., Bassett, D.S., 2009. Reproducibility of graph metrics of human brain functional networks. Neuroimage 47, 1460–1468.
Filippini, N., Ebmeier, K.P., MacIntosh, B.J., Trachtenberg, A.J., Frisoni, G.B., Wilcock, G.K., Beckmann, C.F., Smith, S.M., Matthews, P.M., Mackay, C.E., 2011. Differential effects of the APOE genotype on brain function across the lifespan. Neuroimage 54, 602–610.
Filippini, N., MacIntosh, B., Hough, M., Goodwin, G., Frisoni, G., Smith, S., Matthews, P., Beckmann, C., Mackay, C., 2009. Distinct patterns of brain activity in young carriers of the APOE-ε4 allele. Proc. Natl. Acad. Sci. U. S. A 106, 7209–7214.
Folstein, M.F., Folstein, S.E., McHugh, P.R., 1975. "Mini-mental state." A practical method for grading the cognitive state of patients for the clinician. J. Psychiatr. Res. 12, 189–198.
Fornito, A., Zalesky, A., Bullmore, E.T., 2010. Network scaling effects in graph analytic studies of human resting-state FMRI data. Front. Syst. Neurosci. 4, 22.
Freeman, L., 1977. A set of measures of centrality based on betweenness. Sociometry 40, 35–41.
Frisoni, G.B., Testa, C., Sabattoli, F., Beltramello, A., Soininen, H., Laakso, M.P., 2005. Structural correlates of early and late onset Alzheimer's disease: voxel based morphometric study. J. Neurol. Neurosurg. Psychiatry 76, 112–114.
Gong, G., He, Y., Chen, Z.J., Evans, A.C., 2012. Convergence and divergence of thickness correlations with diffusion connections across the human cerebral cortex. Neuroimage 59, 1239–1248.
Gong, G., Rosa-Neto, P., Carbonell, F., Chen, Z.J., He, Y., Evans, A.C., 2009b. Age- and gender-related differences in the cortical anatomical network. J. Neurosci. 29, 15684–15693.
Gratton, C., Nomura, E.M., Perez, F., D'Esposito, M., 2012. Focal brain lesions to critical locations cause widespread disruption of the modular organization of the brain. J. Cogn. Neurosci. 24, 1275–1285.
Greicius, M.D., Kimmel, D.L., 2012. Neuroimaging insights into network-based neurodegeneration. Curr. Opin. Neurol. 25, 727–734.
Guimera, R., Amaral, L., 2005. Functional cartography of complex metabolic networks. Nature 433, 895–900.
Hagmann, P., Kurant, M., Gigandet, X., Thiran, P., Wedeen, V.J., Meuli, R., Thiran, J.-P., 2007. Mapping human whole-brain structural networks with diffusion MRI. PLoS One 2, e597.
He, Y., Chen, Z., Gong, G., Evans, A., 2009. Neuronal networks in Alzheimer's disease. Neuroscientist 15, 333–350.
He, Y., Chen, Z., Evans, A., 2008. Structural insights into aberrant topological patterns of large-scale cortical networks in Alzheimer's disease. J. Neurosci. 28, 4756–4766.
Hillebrand, A., Barnes, G.R., Bosboom, J.L., Berendse, H.W., Stam, C.J., 2012. Frequency-dependent functional connectivity within resting-state networks: an atlas-based MEG beamformer solution. Neuroimage 59, 3909–3921.
Honey, C.J., Kötter, R., Breakspear, M., Sporns, O., 2007. Network structure of cerebral cortex shapes functional connectivity on multiple time scales. Proc. Natl. Acad. Sci. U. S. A 104, 10240–10245.
Honey, C.J., Sporns, O., 2008. Dynamical consequences of lesions in cortical networks. Hum. Brain Mapp. 29, 802–809.
Honey, C.J., Sporns, O., Cammoun, L., Gigandet, X., Thiran, J.P., Meuli, R., Hagmann, P., 2009. Predicting human resting-state functional connectivity from structural connectivity. Proc. Natl. Acad. Sci. U. S. A 106, 2035–2040.
Honey, C.J., Thivierge, J.P., Sporns, O., 2010. Can structure predict function in the human brain? Neuroimage 52, 766–776.
Horwitz, B., Rowe, J.B., 2011. Functional biomarkers for neurodegenerative disorders based on the network paradigm. Prog. Neurobiol. 95, 505–509.
Jack Jr., C.R., Knopman, D.S., Jagust, W.J., Shaw, L.M., Aisen, P.S., Weiner, M.W., Petersen, R.C., Trojanowski, J.Q., 2010. Hypothetical model of dynamic biomarkers of the Alzheimer's pathological cascade. Lancet Neurol. 9, 119–128.
Jagust, W.J., Mormino, E.C., 2011. Lifespan brain activity, β-amyloid, and Alzheimer's disease. Trends. Cogn. Sci. 15, 520–526.
Jones, D.T., Vemuri, P., Murphy, M.C., Gunter, J.L., Senjem, M.L., Machulda, M.M., Przybelski, S.A., Gregg, B.E., Kantarci, J.L., Knopman, D.S., Boeve, B.F., Petersen, R.C., Jack Jr., C.R., 2012. Non-stationarity in the "resting brain's" modular architecture. PLoS One 7, e39731.
Karas, G., Scheltens, P., Rombouts, S., Schijndel, R., Klein, M., Jones, B., Flier, W., Vrenken, H., Barkhof, F., 2007. Precuneus atrophy in early-onset Alzheimer's disease: a morphometric structural MRI study. Neuroradiol. 49, 967–976.
Latora, V., Marchiori, M., 2001. Efficient behavior of small-world networks. Phys. Rev. Lett. 87, 198701.
Lehmann, M., Koedam, E.L., Barnes, J., Bartlett, J.W., Ryan, N.S., Pijnenburg, Y.A.L., Barkhof, F., Wattjes, M.P., Scheltens, P., Fox, N.C., 2012. Posterior cerebral atrophy in the absence of medial temporal lobe atrophy in pathologically-confirmed Alzheimer's disease. Neurobiol. Aging 33, 627.e1–627.e12.
Li, Y., Wang, Y., Wu, G., Shi, F., Zhou, L., Lin, W., Shen, D., 2012. Discriminant analysis of longitudinal cortical thickness changes in Alzheimer's disease using dynamic and network features. Neurobiol. Aging 33, 427.e15–427.e30.
Liang, X., Wang, J., Yan, C., Shu, N., Xu, K., Gong, G., He, Y., 2012. Effects of different correlation metrics and preprocessing factors on small-world brain functional networks: a resting-state functional MRI study. PLoS One 7, e32766.
Liu, Z., Zhang, Y., Yan, H., Bai, L., Dai, R., Wei, W., Zhong, C., Xue, T., Wang, H., Feng, Y., You, Y., Zhang, X., Tian, J., 2012. Altered topological patterns of brain networks in mild cognitive impairment and Alzheimer's disease: a resting-state fMRI study. Psychiatry Res. 202, 118–125.

Lo, C.Y., Wang, P.N., Chou, K.H., Wang, J., He, Y., Lin, C.P., 2010. Diffusion tensor tractography reveals abnormal topological organization in structural cortical networks in Alzheimer's disease. J. Neurosci. 30, 16876–16885.
Luce, R.D., Perry, A.D., 1949. A method of matrix analysis of group structure. Psychometrika 14, 95–116.
Maslov, S., Sneppen, K., 2002. Specificity and stability in topology of protein networks. Science 296, 910–913.
Meunier, D., Achard, S., Morcom, A., Bullmore, E., 2009. Age-related changes in modular organization of human brain functional networks. Neuroimage 44, 715–723.
Newman, M.E., 2002. Assortative mixing in networks. Phys. Rev. Lett. 89, 208701.
Newman, M.E., 2003. The structure and function of complex networks. Siam Rev. 45, 167–256.
Onnela, J.P., Saramäki, J., Kertész, J., Kaski, K., 2005. Intensity and coherence of motifs in weighted complex networks. Phys. Rev. E. Stat. Nonlin. Soft Matter Phys. 71, 065103.
Paster-Satorras, R., Vespignani, A., 2001. Epidemic spreading in scale-free networks. Phys. Rev. Lett. 86, 3200–3203.
Pearson, R.C., Esiri, M.M., Hiorns, R.W., Wilcock, G.K., Powell, T.P., 1985. Anatomical correlates of the distribution of the pathological changes in the neocortex in Alzheimer disease. Proc. Natl. Acad. Sci. U. S. A 82, 4531–4534.
Petersen, R.C., Smith, G.E., Waring, S.C., Ivnik, R.J., Tangalos, E.G., Kokmen, E., 1999. Mild cognitive impairment: clinical characterization and outcome. Arch. Neurol. 56, 303–308.
Power, J.D., Barnes, K.A., Snyder, A.Z., Schlaggar, B.L., Petersen, S.E., 2012. Spurious but systematic correlations in functional connectivity MRI networks arise from subject motion. Neuroimage 59, 2142–2154.
Price, C., Friston, K., 2002. Degeneracy and cognitive anatomy. Trends Cogn. Sci. 6, 416–421.
Raj, A., Kuceyeski, A., Weiner, M., 2012. A network diffusion model of disease progression in dementia. Neuron 73, 1204–1215.
Ravasz, E., Barabasi, A.L., 2003. Hierarchical organization in complex networks. Phys. Rev. E Stat. Nonlin. Soft Matter Phys. 67 (2 pt. 2), 026112.
Ridgway, G.R., Lehmann, M., Barnes, J., Rohrer, J.D., Warren, J.D., Crutch, S.J., Fox, N.C., 2012. Early-onset Alzheimer disease clinical variants: multivariate analyses of cortical thickness. Neurology 79, 80–84.
Rubinov, M., Sporns, O., 2010. Complex network measures of brain connectivity: uses and interpretations. Neuroimage 52, 1059–1069.
Sanz-Arigita, E.J., Schoonheim, M.M., Damoiseaux, J.S., Rombouts, S.A., Maris, E., Barkhof, F., Scheltens, P., Stam, C.J., 2010. Loss of 'small-world' networks in Alzheimer's disease: graph analysis of fMRI resting-state functional connectivity. PLoS One 5, e13788.
Seeley, W.W., Crawford, R.K., Zhou, J., Miller, B.L., Greicius, M.D., 2009. Neurodegenerative diseases target large-scale human brain networks. Neuron 62, 42–52.
Sepulcre, J., Sabuncu, M.R., Johnson, K.A., 2012. Network assemblies in the functional brain. Curr. Opin. Neurol. 25, 384–391.
Shao, J., Myers, N., Yang, Q., Feng, J., Plant, C., Böhm, C., Förstl, H., Kurz, A., Zimmer, C., Meng, C., Riedl, V., Wohlschläger, A., Sorg, C., 2012. Prediction of Alzheimer's disease using individual structural connectivity networks. Neurobiol. Aging 33, 2756–2765.
Sheline, Y.I., Morris, J.C., Snyder, A.Z., Price, J.I., Yan, Z., D'Angelo, G., Liu, C., Dixit, S., Benzinger, T., Fagan, A., Mintun, M.A., 2010. APOE4 allele disrupts resting state fMRI connectivity in the absence of amyloid plaques or decreased CSF Aβ42. J. Neurosci. 30, 17035–17040.
Shu, N., Liang, Y., Li, H., Zhang, J., Li, X., Wang, L., He, Y., Wang, Y., Zhang, Z., 2012. Disrupted topological organization in white matter structural networks in amnestic mild cognitive impairment: relationship to subtype. Radiology 265, 518–527.
Smith, S.M., Miller, K.L., Salimi-Khorshidi, G., Webster, M., Beckmann, C.F., Nichols, T.E., Ramsey, J.D., Woolrich, M.W., 2011. Network modelling methods for FMRI. Neuroimage 54, 875–891.
Smits, L., Pijnenburg, Y., Koedam, E., van der Vlies, A.E., Reuling, I.E., Koene, T., Teunissen, C.E., Scheltens, P., van der Flier, W.M., 2012. Early onset Alzheimer's disease is associated with a distinct neuropsychological profile. J. Alzheimers Dis. 30, 101–108.
Solé, R., Valverde, S., 2004. Information theory of complex networks: on evolution and architectural constraints. Lect. Notes Phys. 650, 189–207.
Sperling, R.A., LaViolette, P.S., O'Keefe, K., O'Brien, J., Rentz, D.M., Pihlajamaki, M., Marshall, G., Hyman, B.T., Selkoe, D.J., Hedden, T., Buckner, R.L., Becker, J.A., Johnson, K.A., 2009. Amyloid deposition is associated with impaired default network function in older persons without dementia. Neuron 63, 178–188.
Sporns, O., 2011. The non-random brain: efficiency, economy, and complex dynamics. Front. Comput. Neurosci. 5, 5.
Sporns, O., 2013. Network attributes for segregation and integration in the human brain [e-pub ahead of print]. Curr. Opin. Neurobiol. http://dx.doi.org/10.1016/j.conb.2012.11.015. Accessed at 15 Jan. 2013.
Sporns, O., Tononi, G., Kötter, R., 2005. The human connectome: a structural description of the human brain. PLoS Comp. Biol. 1, e42.
Stam, C.J., de Haan, W., Daffertshofer, A., Jones, B.F., Manshanden, I., van Cappellen van Walsum, A.M., Montez, T., Verbunt, J.P.A., De Munck, J.C., van Dijk, B.W., Berendse, H.W., Scheltens, P., 2009. Graph theoretical analysis of magnetoencephalographic functional connectivity in Alzheimer's disease. Brain 132, 213–224.
Stam, C.J., Hillebrand, A., Wang, H., Van Mieghem, P., 2010. Emergence of modular structure in a large-scale brain network with interactions between dynamics and connectivity. Front. Comput. Neurosci. 4, 133.
Stam, C.J., Jones, B.F., Nolte, G., Breakspear, M., Scheltens, P., 2007. Small-world networks and functional connectivity in Alzheimer's disease. Cereb. Cortex 17, 92–99.
Stam, C.J., Reijneveld, J.C., 2007. Graph theoretical analysis of complex networks in the brain. Nonlinear Biomed. Phys. 1, 3.
Stam, C.J., van Straaten, E.C., 2012. The organization of physiological brain networks. Clin. Neurophysiol. 123, 1067–1087.
Supekar, K., Menon, V., Rubin, D., Musen, M., Greicius, M.D., 2008. Network analysis of intrinsic functional brain connectivity in Alzheimer's disease. PLoS Comp. Biol. 4, e1000100.
Takahashi, R.H., Capetillo-Zarate, E., Lin, M.T., Milner, T.A., Gouras, G.K., 2010. Co-occurrence of Alzheimer's disease β-amyloid and tau pathologies at synapses. Neurobiol. Aging 31, 1145–1152.
Telesford, Q.K., Morgan, A.R., Hayasaka, S., Simpson, S.L., Barret, W., Kraft, R.A., Mozolic, J.L., Laurienti, P.J., 2010. Reproducibility of graph metrics in fMRI networks. Front. Neuroinform. 4, 117.
Tijms, B.M., Möller, C., Vrenken, H., Wink, A.M., de Haan, W., van der Flier, W.M., Stam, C.J., Scheltens, P., Barkhof, F., 2013. Single-subject grey matter graphs in Alzheimer's disease. PLoS One 8, e58921.
Tijms, B.M., Series, P., Willshaw, D.J., Lawrie, S.M., 2012. Similarity-based extraction of individual networks from gray matter MRI scans. Cereb. Cortex 22, 1530–1541.
Tononi, G., Sporns, O., Edelman, G., 1999. Measures of degeneracy and redundancy in biological networks. Proc. Natl. Acad. Sci. U. S. A 96, 3257–3262.
Toppi, J., De Vico Fallani, F., Vecchiato, G., Maglione, A.G., Cincotti, F., Mattia, D., Salinari, S., Babiloni, F., Astolfi, L., 2012. How the statistical validation of functional connectivity patterns can prevent erroneous definition of small-world properties of a brain connectivity network. Comput. Math. Methods Med. 2012, 130985.
Trachtenberg, A.J., Filippini, N., Ebmeier, K.P., Smith, S.M., Karpe, F., Mackay, C.E., 2012. The effects of APOE on the functional architecture of the resting brain. Neuroimage 59, 565–572.
Tzourio-Mazoyer, N., Landeau, B., Papathanassiou, D., Crivello, F., Etard, O., Delcroix, N., Mazoyer, B., Joliot, M., 2002. Automated anatomical labeling of activations in SPM using a macroscopic anatomical parcellation of the MNI MRI single-subject brain. Neuroimage 15, 273–289.
Vaessen, M.J., Hofman, P.A., Tijssen, H.N., Aldenkamp, A.P., Jansen, J.F., Backes, W.H., 2010. The effect and reproducibility of different clinical DTI gradient sets on small world brain connectivity measures. Neuroimage 51, 1106–1116.
van den Heuvel, M.P., Kahn, R.S., Goñi, J., Sporns, O., 2012. High-cost, high-capacity backbone for global brain communication. Proc. Natl. Acad. Sci. U. S. A 109, 11372–11377.
van den Heuvel, M.P., Sporns, O., 2011. Rich-club organization of the human connectome. J. Neurosci. 31, 15775–15786.
van den Heuvel, M.P., Stam, C.J., Boersma, M., Hulshoff Pol, H.E., 2008. Small-world and scale-free organization of voxel-based resting-state functional connectivity in the human brain. Neuroimage 43, 528–539.
van der Flier, W.M., Pijnenburg, Y.A.L., Fox, N.C., Scheltens, P., 2011. Early-onset versus late-onset Alzheimer's disease: the case of the missing APOE ε4 allele. Lancet 10, 280–288.
van Dijk, K.R., Sabuncu, M.R., Buckner, R.L., 2012. The influence of head motion on intrinsic functional connectivity MRI. Neuroimage 59, 431–438.
van Wijk, B.C., Stam, C.J., Daffertshofer, A., 2010. Comparing brain networks of different size and connectivity density using graph theory. PLoS One 5, e13701.
Wang, J., Zuo, X., Dai, Z., Xia, M., Zhao, Z., Zhao, X., Jia, J., Han, Y., He, Y., 2012. Disrupted functional brain connectome in individuals at risk for Alzheimer's disease. Biol. Psychiatry 73, 472–481.
Wang, J.H., Zuo, X.N., Gohel, S., Milham, M.P., Biswal, B.B., He, Y., 2011. Graph theoretical analysis of functional brain networks: test-retest evaluation on short- and long-term resting-state functional MRI data. PLoS One 6, e21976.
Wang, L., Li, Y., Metzak, P., He, Y., Woodward, T.S., 2010. Age-related changes in topological patterns of large-scale brain functional networks during memory encoding and recognition. Neuroimage 50, 862–872.
Watts, D., Strogatz, S., 1998. Collective dynamics of "small-world" networks. Nature 393, 440–442.
Wee, C.Y., Yap, P.T., Li, W., Denny, K., Browndyke, J.N., Potter, G.G., Welsh-Bohmer, K.A., Wang, L., Shen, D., 2011. Enriched white matter connectivity networks for accurate identification of MCI patients. Neuroimage 54, 1812–1822.
Wee, C.Y., Yap, P.T., Zhang, D., Denny, K., Browndyke, J.N., Potter, G.G., Welsh-Bohmer, K.A., Wang, L., Shen, D., 2012. Identification of MCI individuals using structural and functional connectivity networks. Neuroimage 59, 2045–2056.
Wen, W., Zhu, W., He, Y., Kochan, N., Reppermund, S., Slavin, M.J., Brodaty, H., Crawford, J., Xia, A., Sachdev, P., 2011. Discrete neuroanatomical networks are associated with specific cognitive abilities in old age. J. Neurosci. 31, 1204–1212.
Xie, T., He, Y., 2012. Mapping the Alzheimer's brain with connectomics. Front. Psychiatry 2, 77.
Yao, Z., Zhang, Y., Lin, L., Zhou, Y., Xu, C., Jiang, T., Alzheimer's Disease Neuroimaging Initiative, 2010. Abnormal cortical networks in mild cognitive impairment and Alzheimer's disease. PLoS Comp. Biol. 6, e1001006.
Zalesky, A., Fornito, A., Harding, I.H., Cocchi, L., Yücel, M., Pantelis, C., Bullmore, E.T., 2010. Whole-brain anatomical networks: does the choice of nodes matter? Neuroimage 50, 970–983.

Zhao, X., Liu, Y., Wang, X., Liu, B., Xi, Q., Guo, Q., Jiang, H., Jiang, T., Wang, P., 2012. Disrupted small-world brain networks in moderate Alzheimer's disease: a resting-state fMRI study. PLoS One 7, e33540.

Zhou, J., Gennatas, E.D., Kramer, J.H., Miller, B.L., Seeley, W.W., 2012. Predicting regional neurodegeneration from the healthy brain functional connectome. Neuron 73, 1216–1227.

Zhou, J., Greicius, M.D., Gennatas, E.D., Growdon, M.E., Jang, J.Y., Rabinovici, G.D., Kramer, J.H., Weiner, M., Miller, B.L., Seeley, W.W., 2010. Divergent network connectivity changes in behavioural variant frontotemporal dementia and Alzheimer's disease. Brain 133, 1352–1367.

Zhou, L., Wang, Y., Li, Y., Yap, P.-T., Shen, D., Alzheimer's Disease Neuroimging Initiative, 2011. Hierarchical anatomical brain networks for MCI prediction: revisiting volumetric measures. PLoS One 6, e21935.

Zhu, W., Wen, W., He, Y., Xia, A., Anstey, K.J., Sachdev, P., 2012. Changing topological patterns in normal aging using large-scale structural networks. Neurobiol. Aging 33, 899–913.